TR: MS MGK-P2X

Original Articles are full length reports of original work

Characterization of functional $P2X_1$ receptors in mouse megakaryocytes

Masahiro Ikeda

from

Department of Veterinary Pharmacology, Faculty of Agriculture,

University of Miyazaki, Miyazaki 889-2192, Japan

(4,755 words)

Mailing address

Masahiro Ikeda, D.V.M., Ph.D.

Department of Veterinary Pharmacology, Faculty of Agriculture, University of Miyazaki,

Gakuenkibanadai-nishi 1-1, Miyazaki 889-2192, Japan

TEL **(81) 985 (58) 7268**

FAX **(81) 985 (58) 7268**

e-mail **a0d302u@cc.miyazaki-u.ac.jp**

Abstract

Introduction: Although accumulating evidence within the past five years strongly supports the importance of platelet $P2X_1$ receptors in hemostasis and thrombosis, $P2X_1$ receptors of platelet and /or its progenitor cell, megakaryocyte, have not been fully characterized. The aim of this study was to electrophysiologically and pharamacologically characterize the functional $P2X_1$ receptors on mouse megakaryocytes.

Materials and Methods: The currents in response to nucleotides were examined using the patch-clamp whole-cell recording.

Results: The agonist profile of megakaryocyte $P2X_1$ receptors was ATP > α,β-methyleneATP > β,γ-methyleneATP. The $P2X_1$ receptors exhibited substantial monovalent as well as divalent cation permeability and the ratios of Na^+ to Cs^+ and Ca^{2+} to Cs^+ permeability were 1 and 2.5, respectively. P2X receptor antagonists except suramin significantly inhibited the $P2X_1$ responses with an IC_{50} values of 0.4 μM for pyridoxal-phosphate-6-azophenyl-2',4'-disulphonate (PPADS), 0.3 μM for 2',3'-O-(2,4,6-trinitophenyl)- adenosine 5'-triphosphate (TNP-ATP), 20 μM for reactive blue 2 (RB2), or 160 μM for 8,8'-(carbonylbis(imino-3,1-phenylene carbonylimino)bis(1,3,5-naphthalenetrisulfonic acid) (NF023), respectively. Suramin had no significant effect on the $P2X_1$ responses. In rat megakaryocytes, suramin similarly had no significant effect on the $P2X_1$ responses, but abolished the P2Y receptor-mediated responses, indicating that the suramin was active under present experimental condition.

Conclusions: These results provide the basic properties of mouse megakryocyte $P2X_1$ receptors and would be helpful to examine the P2 receptor signaling in platelets and megakaryocytes. (220 words)

Keywords: megakaryocytes; platelets; ATP; $P2X_1$; patch-clamp

Abbreviations: αβ-meATP, α,β-methyleneATP; βγ-meATP, β,γ-methyleneATP; EGTA, ethylene glycol bis(β-aminoethylether)-N,N,N',N'-tetraacetic acid; ES, external solution; IS, internal solution; NF023, 8,8'-(carbonylbis(imino-3,1-phenylene carbonylimino)bis(1,3,5-naphthalenetrisulfonic acid); PPADS, pyridoxal-phosphate-6-azophenyl-2',4'-disulphonate; RB2, reactive blue 2; SEM, standard error of the mean; TNP-ATP, 2',3'-O-(2,4,6-trinitophenyl)- adenosine 5'-triphosphate.

Introduction

Extracellular adenine nucleotides bind to P2 receptors on the plasma membrane and play an important role in widespread biological responses including platelet aggregation, vascular contraction, neurotransmission, mitosis and apoptosis [1]. Ionotropic P2X receptor is one family of the P2 receptors and on the basis of molecular cloning, seven P2X receptor ($P2X_1$- $P2X_7$) subunits have been identified [2]. These seven homomeric receptors have been characterized electrophysiologically and pharmacologically. The $P2X_1$ and $P2X_3$ receptors are stimulated by the ATP analogue, α,β-methyleneATP (αβ-meATP), and rapidly desensitized even in the continued presence of agonist. In contrast, the other P2X receptors are less sensitive or insensitive to αβ-meATP and do not markedly desensitize [2, 3]. β,γ-methyleneATP (βγ-meATP) is an agonist of $P2X_1$ but not of the $P2X_2$, $P2X_3$ and $P2X_7$ receptors. Suramin and pyridoxal-phosphate-6-azophenyl-2',4'-disulphonate (PPADS) can inhibit the $P2X_1$- $P2X_3$ and $P2X_5$ receptors, but is ineffective or weakly antagonistic towards $P2X_4$, $P2X_6$ and $P2X_7$ receptors[2, 3]. 2',3'-O-(2,4,6-trinitophenyl)-ATP (TNP-ATP) is a potent antagonist of $P2X_1$ and $P2X_3$ receptors [2, 3].

Among seven P2X receptor subunits, $P2X_1$ receptors are known to be expressed in platelets [4, 5]. The role of platelet $P2X_1$ receptors in hemostasis and thrombosis was not defined for many years because of lack of potent and selective $P2X_1$ receptor antagonists and its rapid desensitization property. However, accumulating evidence with specific antagonists and genetically-altered animals within the past five years strongly suggests the importance of platelet $P2X_1$ receptor in thrombosis. Hechler et al. [6] have reported with $P2X_1$-deficient mice that $P2X_1$ receptor contributes to the platelet thrombus formation in small arteries where shear forces are high. This notion was extended by a recent study with the specific $P2X_1$ antagonist, NF449 [7]. Furthermore, studies with transgenic mice over-expressing the $P2X_1$ receptors have revealed that platelet $P2X_1$ receptor plays an important role in collagen- and/or shear stress- mediated hemostasis and thrombosis [8].

Megakaryocytes are the progenitors of platelets. Because the size of megakaryocyte is larger than that of platelet, it is easier to use megakaryocytes for characterizing receptors and ion channels, compared to the tiny, fragile platelets [5]. Indeed, studies with megakaryocytes have helped understand the features of receptors and ion channels of platelets, such as $P2Y_1$ receptors [5, 9-11], Ca^{2+} -dependent K^+ channels [12, 13], inositol 1,4,5-trisphosphate receptors [14] as well as $P2X_1$ receptors

as mentioned below. Thus, certain types of receptors and ion channels in megakaryocytes are now recognized as a bona fide model for those in platelets [5].

So far, in order to characterize platelet/megakaryocyte $P2X_1$ receptors, several studies with megakaryocytes have been performed and these studies have revealed that $P2X_1$ receptors in megakaryocytes are permeable to Ca^{2+}, activated by αβ-meATP, and inhibited by high doses of suramin derivatives [5, 10, 11, 15]. However, a relative Ca^{2+} to monovalent ion permeability ratio is not known and, dose-response relations for agonists and those for atagonists including suramin derivatives remain obscure. In this study, to further characterize platelet/megakaryocyte $P2X_1$ receptors, which include the analysis of agonist and antagonist profiles and relative Ca^{2+} permeability, electrophysiological and pharamacological experiments were conducted. The results show that the most features of the $P2X_1$ receptors on megakaryocytes do match those of the homomeric $P2X_1$ receptors expressed heterologously in *Xenopus laevis* oocytes except the sensitivities to some antagonists including suramin, TNP-ATP, and NF023.

Methods

Cell preparation and solutions

Animals were housed and cared for in accordance with the Guide for the Care and Use of Laboratory Animals [DHEW (DHHS) Publication No. (NIH) 85-23, revised 1996, Office of Science and Health Reports, DRR/NIH, Bethesda, MD 20205]. Procedure using laboratory animals were approved by the Institutional Animal Care and Use Committee of University of Miyazaki. The cell preparation procedure performed in this study was similar to those described previously [9, 14]. Briefly, mouse or rat bone marrow was flushed out with Na^+-rich external solution (Na^+-ES) and dispersed by repetitive pipetting. After removal of large pieces of tissue, the cells were washed twice by gentle centrifugation for a minute and resuspended in Na^+-ES including apyrase (6 U/ml) except for the experiment with TNP-ATP which is known to be degraded by nucleotidases. The cells were used within 2 h of isolation. The Na^+-ES contained 150 mM NaCl, 2 mM $MgCl_2$, and 10 mM HEPES. The pH was adjusted to 7.2 using NaOH.

In order to block the K^+ channels reported to be present on megakaryocytes [13, 16], Cs^+-rich internal solution (Cs^+-IS) was used as an intrapipette solution for whole-cell recording in most studies. The Cs^+-IS contained 150 mM CsCl, 2 mM $MgCl_2$, 1 mM ethylene glycol bis(β-aminoethylether)-N,N,N',N'-tetraacetic acid (EGTA) and 10 mM HEPES. The pH was adjusted to 7.2 using CsOH. K^+-rich internal solution (K^+-IS) with a low-Ca^{2+}-buffer was used as an intrapipette solution only when the effect of suramin on the Ca^{2+}-dependent K^+ channels was studied in rat megakaryocytes. The K^+-IS contained 150 mM KCl, 2 mM $MgCl_2$, 0.1 mM EGTA and 10 mM HEPES. The pH was adjusted to 7.2 using KOH. To measure the permeation of Ca^{2+} through a channel, Ca^{2+}-rich external solution (Ca^{2+}-ES) was used as a bath solution. The Ca^{2+}-ES contained 110 mM $CaCl_2$ and 10 mM HEPES. The pH was adjusted to 7.2 using tetraethylammonium hydroxide. Junction potentials were measured using a 3 M KCl bridge in the bath to eliminate changes in the reference electrode potential. The measured junction potential between Cs^+-IS versus Na^+-ES or Ca^{2+}-ES was about –2 or -6 mV, respectively. The errors caused by junction potentials were corrected as described previously [17].

All chemicals and reagents used in this study were purchased from either Sigma (St. Louis, MO) or Wako Pure Chemicals (Osaka, Japan).

Electrophysiological experiment

The patch-clamp experimental procedures were similar to those described previously [16, 17]. Briefly, the experiments were performed in the tight seal whole-cell configuration (with EPC-7, List, Darmstadt, Germany) at room temperature (around 25˚C). The pipette resistance, after filling with IS, ranged between 2 MΩ and 4 MΩ. Most of the current responses were evaluated at -62 mV. The input capacitance of megakaryocytes used in this study ranged from 60 to 280 pF. The reversal potential was obtained by clamping the cell from a holding potential to a run of three increasing steps in 30 mV increments with 35 ms in duration of each step at 1.5 Hz. The current responses were monitored on a chart recorder (WR7700, Graphtec, Tokyo, Japan) or a PCM data recorder (RD101T, Teac, Yokohama, Japan) through a low-pass filter of 200 Hz.

Drug application

Extracellular ATP or its analogue was puff-applied without apyrase to isolated single megakaryocyte by a nearby pipette of 30-35 μm diameter. Each application was achieved by bringing the pipette to the setting point quickly (within 30 μm of the cell) from outside the bathing solution. The puff pressure was adjusted to achieve agonist application rapidly and effectively. The dose-response relationships for nucleotide-induced currents were determined by administering one dose of nucleotide in one megakaryocyte to avoid any desensitization of the response [18].

To study the effect of externally applied P2 receptor antagonist on the nucleotide-induced responses, two bathing chambers (test and control) were placed on the stage of an inverted microscope (IMT-2, Olympus, Tokyo, Japan). One chamber contained a batch of cells immersed in Na^+-ES containing test materials (test chamber), and the other contained the same batch of cells immersed in Na^+-ES alone (control chamber).

Data analysis

Data are expressed as means ± standard error of the mean (SEM). Statistical comparisons of means between two groups were performed using Student's t-test; Dunnett's method was used to test comparisons of means between three or more groups.

The relative ionic permeability of Ca^{2+} was calculated from the reversal potential using the modified Goldman-Hodgkin-Katz equation. In this calculation, values of 25.2 mV for RT/F, 0.75 for monovalent ion activity and 0.25 for divalent ion activity were used [19].

Results

Dose-response relationships for nucleotide-induced currents

When the cells were immersed in Na^+-ES and the patch pipette contained Cs^+-IS, 0.1, 1 or 10 μM ATP was challenged at a holding potential of -62 mV (Fig. 1A, B & C). At an ATP concentration of 0.01 μM, the current responses were not observed. However, at an ATP concentration of 0.1 μM or more, all of the cells tested responded to ATP. Increasing the dose increased the peak amplitude of the ATP-induced inward currents. The rapid inward current induced by a higher concentration of ATP (1 μM or more) peaked within 100 ms and then decayed in the continued presence of ATP (Fig. 1B & C). The half-decay time, defined as the time to 50% of the peak amplitude of the current from the peak, was about 400 ms at ATP concentrations of 1 and 10 μM.

A similar rapid inward current was also observed when αβ-meATP or βγ-meATP was applied to the cell (Fig. 1E & Fig. 2Aa). However, somewhat reduced maximal currents in response to either αβ-meATP or βγ-meATP were observed compared with the maximum ATP response (Fig. 1E), suggesting that αβ-meATP and βγ-meATP are partial agonists.

UTP (100 μM) is known to activate an inward current in other types of cells [1], but had no effect on the holding (-62 mV) current in mouse megakaryocytes (3 of 3 cells, Fig. 1D).

The means ± SEM of the current amplitude at each dose of nucleotides was plotted against a logarithmic scale of dose (Fig. 1E). After the relative amplitude at each dose of nucleotide had been calculated with reference to the mean maximum response induced by 30 μM ATP, 30 μM αβ-meATP or 1 mM βγ-meATP, each concentration-response relationship was fitted by the Hill equation using the least-squares method as described previously [20]. Based on the relationship, the EC50 values for ATP, αβ-meATP and βγ-meATP were 2.2, 5.9 and 25.4 μM, respectively, and the corresponding Hill coefficients were 0.7, 1.2 and 0.8, respectively.

Current-voltage relationships for nucleotide-induced currents

In preliminary experiments, a ramp-voltage protocol was used to obtain the current-voltage (I-V) relationship for the nucleotide-induced rapid current. However, the nucleotide-induced rapid current during the ramp-protocol was superimposed by a large capacitative current which was due to the large size of the megakaryocyte. Therefore, the I-V relationship was examined by measuring the

nucleotide-induced currents at membrane voltages of –42, -12, 18 and 48 mV. When a megakaryocyte was immersed in Na^+-ES, typical recordings before (open circles) and during (solid circles) application of 30 μM αβ-meATP to the cell are shown in Fig. 2A. Figure 2Ac shows a representative αβ-meATP-sensitive current that is the difference between the solid and open circles in Fig. 2Ab. This recording clearly indicates that the reversal potential for the αβ-meATP-induced current was between –12 and 18 mV. Typical I-V relationships for αβ-meATP- and ATP-induced currents are shown in Fig. 2B. These graphs indicate that each nucleotide-induced current had a mild inward rectification and a reversal potential near 0 mV. The means ± SEM of reversal potentials for the nucleotide-induced currents from three batches of cells were 4.4 ± 2.4 mV for αβ-meATP (n = 8) and 8.3 ± 1.5 mV for ATP (n = 6). From these values, the ratio of Na^+ to Cs^+ permeability was almost 1.

Ca^{2+} permeation for nucleotide-induced currents

The permeability of the channels to Ca^{2+} was then examined. Cells were immersed in Ca^{2+}-ES within 10 min and subsequently stimulated with αβ-meATP (100 μM) or ATP (1 mM), because the nucleotide-induced responses from cells that were bathed in Ca^{2+}-ES for over 10 min could not be detected. A typical example of this experiment is depicted in Fig. 3A. In Ca^{2+}-ES, the amplitude of each nucleotide-induced current seemed reduced compared with that observed in Na^+-ES (See also Fig. 1 B, 1 C & Fig. 2Aa). The amplitude of the αβ-meATP or ATP-induced current was 92.4 ± 34.8 (n = 7) or 82.5 ± 34.5 pA (n = 5), respectively. Furthermore, with Ca^{2+}-ES, the nucleotide-induced currents had a much slower time course than those observed in Na^+-ES (see also Fig. 1). This depressive phenomenon may have been due to a reduction in the proportion of the free form of nucleotide in this medium and/or inhibition of receptor-agonist binding by a high concentration of Ca^{2+} [18].

Figure 3B demonstrates the typical I-V relationship for the αβ-meATP-induced current under the same voltage-clamp protocol as that shown in Fig. 2. This graph indicates that the αβ-meATP-induced current in Ca^{2+}-ES had mild inward rectification. The mean ± SEM of the reversal potentials for the αβ-meATP-induced currents was 3.3 ± 2.0 mV (n = 3), corresponding to relative selection for Ca^{2+} over Cs^+ of 2.5 according to the modified Goldman-Hodgkin-Katz equation [19].

Effects of suramin and its derivative on nucleotide-induced inward current

The effect of suramin on the nucletotide-induced inward currents was studied. Cells were immersed in Na^+-ES alone or Na^+-ES containing 100 μM or 1 mM suramin for 41-83 min, and subsequently stimulated with ATP (1 μM). Figure 4A summarizes the effect of suramin on the amplitudes of ATP-induced currents. Suramin did not have any inhibitory effect on the current.

NF023, a derivative of suramin [2, 21], was examined. Figure 4B shows an example of paired control and test recordings, obtained from the same batch of cells, and Fig.4C summarizes the effects of NF023 on the amplitudes of ATP-induced currents. NF023 reduced ATP-induced currents in a dose-dependent manner with an IC50 value of 160 μM.

Suramin is known to be an inhibitor of ecto-nucleotidase [1, 21]. Since αβ-meATP is stable ATP analogue against the nucleotidase, the effect of suramin on the amplitude of αβ-meATP-induced currents was also examined. As shown in Fig. 4D, suramin (1 mM) had no significant effect on the αβ-meATP-induced currents. In this experiment αβ-meATP concentration was 6 μM, because it produced a response comparable to those of 1 μM ATP (Fig. 1E).

Effect of PPADS, TNP-ATP, or RB2 on nucleotide-induced inward current

PPADS is known to inhibit certain types of P2X receptors [1-3, 21]. Figure 5A summarizes the effects of PPADS on the amplitudes of the ATP (1 μM) -induced currents from three batches of cells. PPADS inhibited the ATP–induced currents with an IC50 value of 0.4 μM.

TNP-ATP is known to inhibit homomeric $P2X_1$ and $P2X_3$ receptor [1-3, 21]. Figure 5B summarizes the effects of TNP-ATP on the amplitudes of the ATP (1 μM) -induced currents. TNP-ATP inhibited the ATP–induced currents with an IC50 value of 0.3 μM.

RB2 is a non-competitive P2 receptor antagonist [1, 22]. Figure 5C summarizes the effects of RB2 on the amplitudes of the ATP (1 μM) -induced currents. RB2 inhibited the ATP–induced currents with an IC50 value of 20 μM.

Effect of suramin on ATP-induced currents in rat megakaryocytes

In previous studies with rat megakaryocytes, externally applied ATP induced periodic K^+ channel activation which reflected oscillation of the cytoplasmic free Ca^{2+} concentration [23]. This Ca^{2+} increase was thought to be mediated by a suramin-sensitive P2 receptor coupled to G protein-PLC

system [24]. On the other hand, Kawa has described the failure of mouse megakaryocytes to activate the K^+ channel after exposure to A23187, a calcium ionophore, and commented that this failure was probably due to a low density or complete lack of the Ca^{2+}-dependent K^+ channels on the mouse megakaryocyte plasma membrane [18]. Therefore, in order to determine whether the less sensitivity of $P2X_1$ receptor to suramin is conserved across species and whether suramin can inhibit the P2 receptor coupled to a G protein-PLC system under the present experimental conditions, the effects of suramin on both ATP-induced outward and inward currents of rat megakaryocytes were examined.

When the membrane was held at –42 mV and the patch pipette contained K^+-IS with a low Ca^{2+} buffer, the addition of ATP (10 μM) to the cells immersed in Na^+-ES alone evoked an early small transient inward current followed by an obvious periodic outward current (Fig. 6Aa). The observed pattern of this response was similar in all of the cells tested (6 cells) and was in good agreement with previous report [18]. In contrast, addition of ATP (10 μM) to the cells immersed in Na^+-ES containing suramin evoked only a larger transient inward current. In the presence of suramin, none of the cells tested activated a periodic outward current in response to ATP (4 cells). With K^+-IS, the mean amplitude of the inward current in the presence of suramin (945.3 ± 167 pA, n = 4) was significantly larger than that in its absence (62.0 ± 21.5, n = 6, $P < 0.05$). These results suggest that suramin inhibits the outward current activated through a P2 receptor-G protein-PLC system on rat megakaryocytes.

Next, with Cs^+-IS, the effect of suramin on the ATP-induced inward currents in rat megakaryocytes was examined. When the membrane was held at –42 mV and the patch pipette contained Cs^+-IS, addition of ATP (1 μM) to the cells immersed in Na^+-ES alone evoked a transient inward current. In contrast to with K^+-IS, none of the cells tested activated the outward current with Cs^+-IS (4 cells). The mean ± SEM of the amplitude of the inward current was shown in Fig. 6B. The inward currents with Cs^+-IS in the absence of suramin was obviously larger than that obtained with K^+-IS (Fig. 6Aa), suggesting that superimposition of the outward current on the inward current is responsible for the reduced response to ATP with K^+-IS. With Cs^+-IS, suramin (100 μM) did not have significant effect on the amplitude of the inward current in rat megakaryocytes (Fig. 6B), as shown earlier with mouse megakaryocytes (Fig. 4A).

Discussion

In platelets, the presences of $P2X_1$ receptor protein and mRNA [25-28] as well as the functional inward currents induced by ATP [29-30] were reported. In freshly isolated megakaryocytes that are the progenitors of platelets, ATP and αβ-meATP were also shown to activate rapid inward currents and this current appeared to be involved in a rapid cellular Ca^{2+} increase [15, 31]. Furthermore, RT-PCR studies revealed that no other P2X receptor subunit other than the $P2X_1$ subunit was detected in human platelets [27]. These data strongly suggested that platelet/megakaryocyte lineage expressed functional $P2X_1$ receptors. In 2002, patch clamp studies with megakryocytes from $P2X_1$-deficient mice clearly showed that αβ-meATP-induced rapid inward currents were mediated by $P2X_1$ receptors [10]. The following studies with $P2X_1$-deficient mice also confirmed that $P2X_1$ receptor was only receptor responsible for Ca^{2+} influx in response to αβ-meATP in platelets [6]. Therefore, it is now recognized that $P2X_1$ receptor is only functional isoform among a P2X receptor family in platelet/megakaryocyte lineage.

The homomeric $P2X_1$ receptor has been well-characterized with the *Xenopus laevis* oocyte expression system [1-3, 22]. The heterologously expressed homomeric $P2X_1$ receptor produced the rapid inward current in response to αβ-meATP and then decayed rapidly in the continued presence of αβ-meATP. The agonist profile of the receptor is ATP > αβ-meATP > βγ-meATP with the EC50 values of 0.1-1 μM for ATP, 1-3 μM for αβ-meATP, and 10 μM for βγ-meATP and the corresponding Hill coefficients were 0.8, 0.8 and 0.6, respectively. In the quantitative experiments on Ca^{2+} permeability, heterologously expressed $P2X_1$ receptor is permeable to Ca^{2+} with the relative selection for Ca^{2+} over Na^+ of ~5. In the present study, mouse megakaryocyte $P2X_1$ receptors were characterized. The megakaryocyte $P2X_1$ receptors were rapidly activated and desensitized in response to nucleotides. The agonist profile was ATP > αβ-meATP > βγ-meATP with the EC50 values of 2.2 μM for ATP, 5.9 μM for αβ-meATP, and 25.4 μM for βγ-meATP and the corresponding Hill coefficients were 0.7, 1.2 and 0.8, respectively. The megakaryocyte $P2X_1$ receptors also exhibited substantial Ca^{2+} permeability and the calculated P_{Ca}/P_{Cs} ratio was 2.5. These data clearly show that the properties of the mouse megakaryocyte $P2X_1$ receptor accord closely with the recombinant $P2X_1$ homomeric receptor.

Wildman et al. [22] reported that the both αβ-meATP and βγ-meATP were partial agonists at homomeric rat $P2X_1$ receptors expressed heterologously in *Xenopus laevis* oocytes. In the present

study, the partial agonist profiles of both αβ-meATP and βγ-meATP at mouse megakaryocyte $P2X_1$ receptors were also observed. Again, these data indicate that there is very similarity between the mouse megakaryocyte $P2X_1$ receptor and the homomeric $P2X_1$ receptor.

Antagonist sensitivities at homomeric $P2X_1$ receptors expressed heterologously in *Xenopus laevis* oocytes have also been characterized [1-3, 21, 22]. Suramin, PPADS, TNP-ATP, RB2, and NF023 inhibited the ATP (1 μM)-induced currents with IC50 values of 1-2 μM, 0.1-1 μM, 0.001-0.006 μM, 2.3 μM and 0.2 μM, respectively. These antagonist sensitivities to megakaryocyte $P2X_1$ receptors were examined in the present study and the IC50 value of each antagonist to ATP (1 μM) -induced response was > 1 mM for suramin, 0.4 μM for PPADS, 0.3 μM for TNP-ATP, 20 μM for RB2, or 160 μM for NF023, respectively. These data clearly show the remarkable insensitivities (> 50-fold less potent) of megakaryocyte $P2X_1$ receptors to suramin, TNP-ATP, and NF023, compared with homomeric $P2X_1$ receptors.

It has been reported that TNP-ATP was a very week antagonist of αβ-meATP-induced contraction in rat mesenteric artery rings and the authors described that the reduced potency of TNP-ATP in whole tissue experiments probably reflects the breakdown of TNP-ATP by endogenous nucleotidases [32]. It is not clear whether this is the case for the present result which shows the week antagonistic activity of TNP-ATP for megakaryocyte $P2X_1$ receptors. Since other types of cells including erythrocytes and leukocytes existed in the recording chamber, it is possible that the breakdown of TNP-ATP occurs under the present experimental condition. In order to explore this point further studies are needed.

Suramin analogues are known to be large polyanionic molecules [33]. Actually, NF449, a suramin analogue, has been observed to be 1000-fold less potent in rat vas deferens than in homomeric $P2X_1$ receptors expressed heterologously in *Xenopus laevis* oocytes [33]. Therefore, the loss of suramin analogue activities might be explained by the interaction with various non-P2 receptor sites. However in the experiments for verifying the suramin activity, 100 μM suramin could completely inhibit the P2 receptors coupled to a G protein-PLC system under the present experimental condition (Fig. 6). Therefore it is likely that the insensitivities of megakaryocyte $P2X_1$ receptors to suramin and NF023 do not result from the lowered effective concentrations of the suramin derivatives around megakaryocytes but is caused by an intrinsic feature of murine megakaryocyte $P2X_1$ receptor.

Recently, the IC_{50} values of suramin and NF023 for inhibiting αβ-meATP(1 μM)-induced [Ca^{2+}] increase in human platelets were reported [34]. The reported IC_{50} values were 2.8 μM for suramin and 2.9 μM for NF023, respectively. Even though the NF023 was slightly less potent, the IC_{50} value of suramin is in reasonable agreement with that at homomeric rat $P2X_1$ receptors expressed heterologously in *Xenopus laevis* oocytes [22]. The reason for the apparent loss in potency of suramin and NF023 at mouse megakaryocyte $P2X_1$ receptors compared with the human platelet as well as recombinant homomeric $P2X_1$ receptors, is not clear at present. One possible explanation for this discrepancy is the different plasma membrane structure between megakryocytes and platelets (as well as *Xenopus laevis* oocytes). Megakaryocytes have a well-developed demarcation membrane system which is a large complex of intracytoplasmic channels formed by the invagination of the plasma membrane and this membrane system is thought to be the precursor of the platelet plasma membrane and open canalicular system [5]. If a significant amount of $P2X_1$ receptors localizes on this membrane, polyanionic molecules cannot easily reach to the target molecules. In order to explore this points, further studies including a careful elucidation of the subcellular localization of $P2X_1$ recceptors in megakaryocytes need to be carried out.

In conclusion, this study has characterized the functional $P2X_1$ receptors on native megakaryocytes both pharmacologically and electrophysiologically, and the most features of the $P2X_1$ receptors on megakaryocytes do match those of the homomeric $P2X_1$ receptors expressed heterologously in *Xenopus laevis* oocytes except the sensitivities to some antagonists including suramin, TNP-ATP, and NF023. These results provide the basic properties of mouse megakryocyte $P2X_1$ receptors and would be helpful to investigate P2 receptor signaling in platelets and megakaryocytes.

References

[1] Ralevic V, Burnstock G. Receptors for purines and pyrimidines. Pharmacol Rev 1998; 50:413-92.

[2] North RA. Molecular physiology of P2X receptors. Physiol Rev 2002, 82:1013-67.

[3] North RA, Surprenant A. Pharmacology of cloned P2X receptors. Annu Rev Pharmacol Toxicol 2000; 40:563-80.

[4] Kunapuli SP, Dorsam RT, Kim S, Quinton TM. Platelet purinergic receptors. Curr Opin Pharmacol 2003, 3:175-80.

[5] Mahaut-Smith MP, Tolhurst G, Evans RJ. Emerging roles for $P2X_1$ receptors in platelet activation. Platelets 2004, 15:131-44.

[6] Hechler B, Lenain N, Marchese P, Vial C, Heim V, Freund M, Cazenave JP, Cattaneo M, Ruggeri ZM, Evans R, Gachet C. A role of the fast ATP-gated $P2X_1$ cation channel in thrombosis of small arteries in vivo. J Exp Med 2003, 198:661-7.

[7] Hechler B, Magnenat S, Zighetti ML, Kassack MU, Ullmann H, Cazenave JP, Evans R, Cattaneo M, Gachet C. Inhibition of platelet functions and thrombosis through selective or nonselective inhibition of the platelet P2 receptors with increasing doses of NF449 [4,4',4",4"'-(carbonylbis(imino-5,1,3-benzenetriylbis-(carbonylimino)))tetrakis-benzene-1,3-disulfonic acid octasodium salt]. J Pharmacol Exp Ther 2005, 314:232-43.

[8] Oury C, Kuijpers MJ, Toth-Zsamboki E, Bonnefoy A, Danloy S, Vreys I, Feijge MA, De Vos R, Vermylen J, Heemskerk JW, Hoylaerts MF. Overexpression of the platelet $P2X_1$ ion channel in transgenic mice generates a novel prothrombotic phenotype. Blood 2003, 101:3969-76.

[9] Ikeda M, Kurokawa K, Maruyama Y. Cyclic nucleotide-dependent regulation of agonist-induced calcium increases in mouse megakaryocytes. J Physiol 1992, 447:711-28.

[10] Vial C, Rolf MG, Mahaut-Smith MP, Evans RJ. A study of $P2X_1$ receptor function in murine megakaryocytes and human platelets reveals synergy with P2Y receptors. Br J Pharmacol 2002, 135:363-72.

[11] Tolhurst G, Vial C, Leon C, Gachet C, Evans RJ, Mahaut-Smith MP. Interplay between $P2Y_1$, $P2Y_{12}$, and $P2X_1$ receptors in the activation of megakaryocyte cation influx currents by ADP: evidence that the primary megakaryocyte represents a fully functional model of platelet P2

receptor signaling. Blood 2005, 106:1644-51.

[12] Maruyama Y. A patch-clamp study of mammalian platelets and their voltage-gated potassium current. J Physiol 1987,391:467-85.

[13] Kawa K. Guinea-pig megakaryocytes can respond to external ADP by activating Ca^{2+}-dependent potassium conductance. J Physiol 1990, 431:207-24.

[14] Ikeda M, Maruyama Y. Inhibitory effects of ruthenium red on inositol 1,4, 5-trisphosphate-induced responses in rat megakaryocytes. Biochem Pharmacol 2001, 61:7-13.

[15] Somasundaram B, Mahaut-Smith MP. Three cation influx currents activated by purinergic receptor stimulation in rat megakaryocytes. J Physiol 1994, 480:225-31.

[16] Ikeda M, Kurokawa K, Maruyama Y. Ca^{2+} spike initiation from sensitized inositol 1,4,5-trisphosphate-sensitive Ca^{2+} stores in megakaryocytes. Pflugers Arch 1994, 427:355-64.

[17] Ikeda M, Iyori M, Yoshitomi K, Hayashi M, Imai M, Saruta T, Kurokawa K. Isoproterenol stimulates Cl^- current by a Gs protein-mediated process in beta-intercalated cells isolated from rabbit kidney. J Membr Biol 1993, 136:231-41.

[18] Kawa K. ADP-induced rapid inward currents through Ca^{2+}-permeable cation channels in mouse, rat and guinea-pig megakaryocytes: a patch-clamp study. J Physiol 1996, 495:339-52.

[19] Benham CD, Tsien RW. A novel receptor-operated Ca^{2+}-permeable channel activated by ATP in smooth muscle. Nature 1987, 328:275-8.

[20] Ikeda M, Beitz E, Kozono D, Guggino WB, Agre P, Yasui M. Characterization of aquaporin-6 as a nitrate channel in mammalian cells. Requirement of pore-lining residue threonine 63. J Biol Chem 2002, 277:39873-9.

[21] Lambrecht G. Agonists and antagonists acting at P2X receptors: selectivity profiles and functional implications. Naunyn Schmiedebergs Arch Pharmacol 2000, 362:340-50.

[22] Wildman SS, Brown SG, Rahman M, Noel CA, Churchill L, Burnstock G, Unwin RJ, King BF. Sensitization by extracellular Ca^{2+} of rat $P2X_5$ receptor and its pharmacological properties compared with rat $P2X_1$. Mol Pharmacol 2002, 62:957-66.

[23] Uneyama C, Uneyama H, Akaike N. Cytoplasmic Ca^{2+} oscillation in rat megakaryocytes evoked by a novel type of purinoceptor. J Physiol 1993, 470:731-49.

[24] Uneyama H, Uneyama C, Ebihara S, Akaike N. Suramin and reactive blue 2 are antagonists for a

newly identified purinoceptor on rat megakaryocyte. Br J Pharmacol 1994, 111:245-9.

[25] Vial C, Hechler B, Leon C, Cazenave JP, Gachet C. Presence of $P2X_1$ purinoceptors in human platelets and megakaryoblastic cell lines. Thromb Haemost 1997, 78:1500-4.

[26] Clifford EE, Parker K, Humphreys BD, Kertesy SB, Dubyak GR. The $P2X_1$ receptor, an adenosine triphosphate-gated cation channel, is expressed in human platelets but not in human blood leukocytes. Blood 1998, 91:3172-81.

[27] Sun B, Li J, Okahara K, Kambayashi J. $P2X_1$ purinoceptor in human platelets. Molecular cloning and functional characterization after heterologous expression. J Biol Chem 1998, 273:11544-7.

[28] Scase TJ, Heath MF, Allen JM, Sage SO, Evans RJ. Identification of a P_{2X1} purinoceptor expressed on human platelets. Biochem Biophys Res Commun 1998, 242:525-8.

[29] Mahaut-Smith MP, Sage SO, Rink TJ. Rapid ADP-evoked currents in human platelets recorded with the nystatin permeabilized patch technique. J Biol Chem 1992, 267:3060-5.

[30] MacKenzie AB, Mahaut-Smith MP, Sage SO. Activation of receptor-operated cation channels via P_{2X1} not P_{2T} purinoceptors in human platelets. J Biol Chem 1996, 271:2879-81.

[31] Mahaut-Smith MP, Ennion SJ, Rolf MG, Evans RJ. ADP is not an agonist at $P2X_1$ receptors: evidence for separate receptors stimulated by ATP and ADP on human platelets. Br J Pharmacol 2000, 131:108-14.

[32] Lewis CJ, Surprenant A, Evans RJ. 2',3'-O-(2,4,6- trinitrophenyl) adenosine 5'-triphosphate (TNP-ATP)--a nanomolar affinity antagonist at rat mesenteric artery P2X receptor ion channels. Br J Pharmacol 1998, 124:1463-6.

[33] Braun K, Rettinger J, Ganso M, Kassack M, Hildebrandt C, Ullmann H, Nickel P, Schmalzing G, Lambrecht G. NF449: a subnanomolar potency antagonist at recombinant rat $P2X_1$ receptors. Naunyn Schmiedebergs Arch Pharmacol 2001, 364:285-90.

[34] Horner S, Menke K, Hildebrandt C, Kassack MU, Nickel P, Ullmann H, Mahaut-Smith MP, Lambrecht G. The novel suramin analogue NF864 selectively blocks $P2X_1$ receptors in human platelets with potency in the low nanomolar range. Naunyn Schmiedebergs Arch Pharmacol 2005, 372:1-13.

Figure legends

Fig. 1.

Inward currents evoked by externally applied nucleotides

Currents were recorded in Na^+-rich external solution (Na^+-ES) using a whole-cell patch electrode containing Cs^+-rich internal solution (Cs^+-IS) at a holding potential of –62 mV. Nucleotide was applied during the time indicated by the bar above each trace. (A-C) Typical examples of ATP-induced inward currents. Applied doses of ATP were 0.1 (A), 1 (B) and 10 μM (C). (D) A typical recording when UTP (100 μM) was applied to a megakaryocyte. UTP had no effect on the holding current. (E) Dose-response relationships for ATP (open circle), αβ-meATP (solid circle) , βγ-meATP (solid triangle), and UTP (solid square). Symbols are means of the peak amplitudes and vertical lines show SEM. Sigmoidal lines represent the best fit to a least-square curve-fitting routine [20]. Numbers in parentheses are the numbers of cells tested.

Fig. 2.

Current-voltage relationships of the nucleotide-induced currents

(A) A typical recording in which application of αβ-meATP (30 μM) evoked a rapid inward current to membrane voltage. The cell was held at –42 mV and a series of three voltage steps whose protocol was shown in (b) were applied every 0.75 s. The bar above the trace in (a) indicates the application of αβ-meATP. Open and solid circles denote the before and during the application of αβ-meATP, respectively, during the series of three voltage steps on the holding potential. The arrowhead in (a) indicates the level of the holding current. The current trace of (a) is presented with a faster time scale in (b). The rectangular line above the trace represents the voltage clamp protocol. Open and closed circles correspond with those in (a). The dotted line is the zero current level. The arrows indicate the holding current levels before and after the series of three voltage steps at solid circle and almost the same level of the arrows indicate that the contamination of the receptor desensitization on the current responses during the voltage steps is minimum. (c) The αβ-meATP-induced current is expressed as the difference between the currents before (open circle) and during (solid circle) addition of αβ-meATP. The dotted line is the zero current level. (B) Typical examples of current-voltage relations of nucleotide-induced currents (a, 30 μM αβ-meATP; b, 20 μM ATP) measured at the ends of the voltage steps. The voltage

protocol was the same as in (A). Each point was plotted after leakage subtraction (see Ac).

Fig. 3.

Nucleotide-induced currents in Ca^{2+}-rich external solution

(A) Typical recordings of αβ-meATP (a) and ATP (b)-induced inward currents. Currents were recorded in Ca^{2+}-rich external solution (Ca^{2+}-ES) using a whole-cell patch electrode containing Cs^{+}-IS at a holding potential of –46 mV. Applied doses of αβ-meATP and ATP were 100 μM and 1 mM, respectively. Nucleotide was applied during the time indicated by the bar above each trace. The upper end of the vertical scale bar is the zero current level. Preincubation of cells with Ca^{2+}-ES had no effect on the holding current. (B) A typical αβ-meATP-induced current-voltage relation, representing 3 megakaryocytes. The voltage protocol was the same as in Fig. 2A. Each point was plotted after leakage subtraction.

Fig. 4.

Effects of suramin and NF023 on nucleotide-induced currents

(A) Effect of suramin on ATP-induced currents is summarized. Symbols are means of the peak amplitudes and vertical lines show SEM. Applied dose of ATP was 1 μM. (B) Typical recordings of ATP-induced inward currents in the absence (a) or presence of NF023 (b). (C) Effect of NF023 on ATP-induced currents is summarized. Symbols are means of the peak amplitudes and vertical lines show SEM. Applied dose of ATP was 1 μM. (D) Effect of suramin on αβ-meATP-induced currents is summarized. Values are presented as mean ± SEM. Applied dose of αβ-meATP was 6 μM. Numbers in parentheses are the numbers of cells tested. $*P < 0.05$ and $***P < 0.001$ vs. response in the absence of drug (Dunnett's method). NS, not significant (Student's t-test)

Fig. 5.

Effects of PPADS, TNP-ATP and RB2 on ATP-induced currents

Effects of PPADS (A), TNP-ATP (B) and RB2 (C) on ATP-induced currents are summarized. Symbols are means of the peak amplitudes and vertical lines show SEM. Applied dose of ATP was 1 μM. Numbers in parentheses are the numbers of cells tested. $*P < 0.05$ and $***P < 0.001$ vs. response in the absence of drug (Dunnett's method).

Fig. 6.

Effects of suramin on ATP-induced currents in rat megakaryocytes

(A) Typical recordings of ATP-induced currents using a whole-cell patch electrode containing K^+-IS at a holding potential of –62 mV in Na^+-ES alone (a) or Na^+-ES containing 100 μM suramin (b). Applied dose of ATP was 10 μM. (B) Data from the ATP-induced inward current recordings using a whole-cell patch electrode containing Cs^+-IS in Na^+-ES alone (a) or Na^+-ES containing 100 μM suramin (b) are summarized. Applied dose of ATP was 1 μM. Numbers in parentheses are the numbers of cells tested. NS, not significant (Student's t-test).

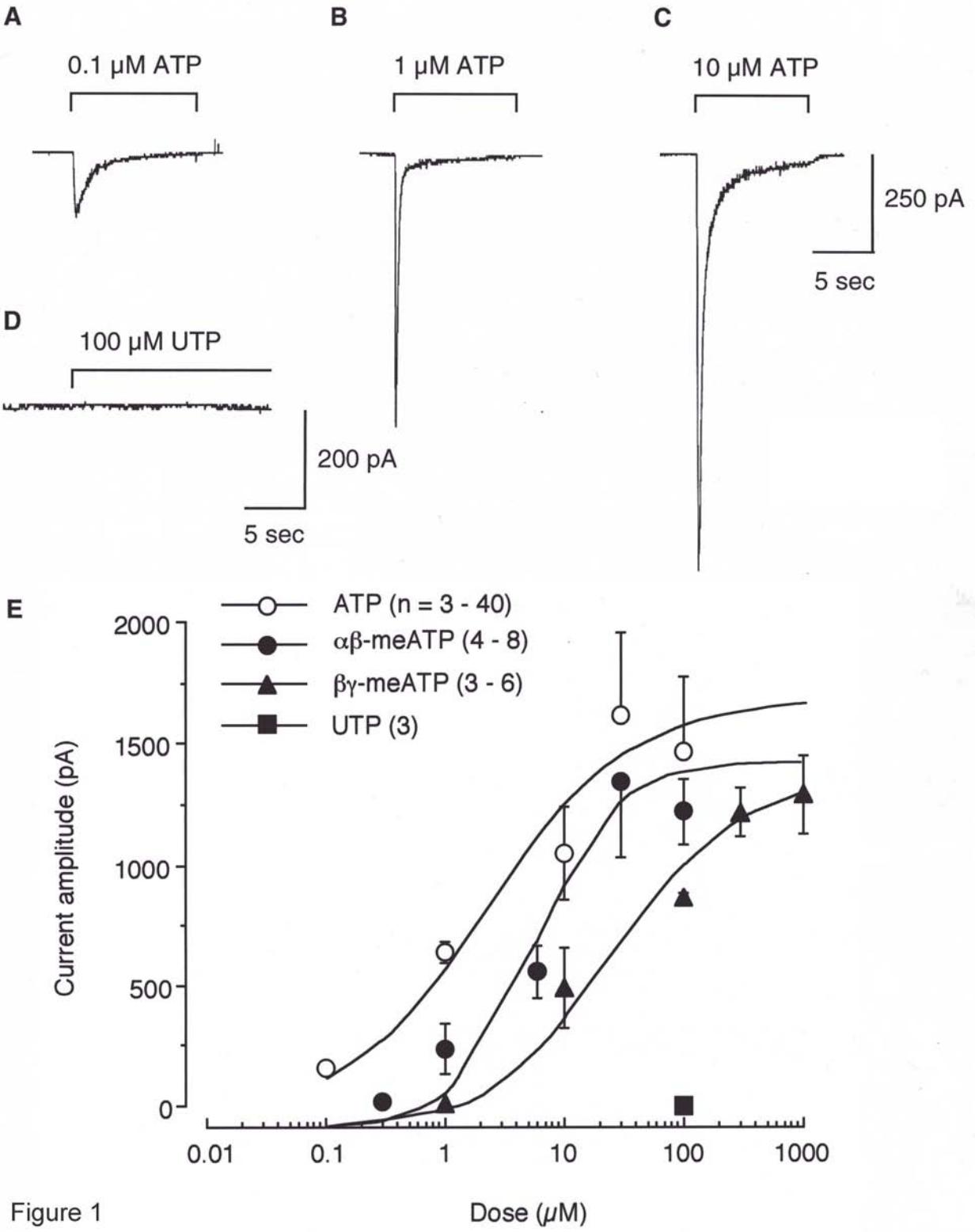
A
0.1 μM ATP
B
1 μM ATP
C
10 μM ATP
250 pA
5 sec
D
100 μM UTP
200 pA
5 sec
E
ATP (n = 3 - 40)
αβ-meATP (4 - 8)
βγ-meATP (3 - 6)
UTP (3)
Current amplitude (pA)
2000
1500
1000
500
0
0.01
0.1
1
10
100
1000
Dose (μM)

Figure 1

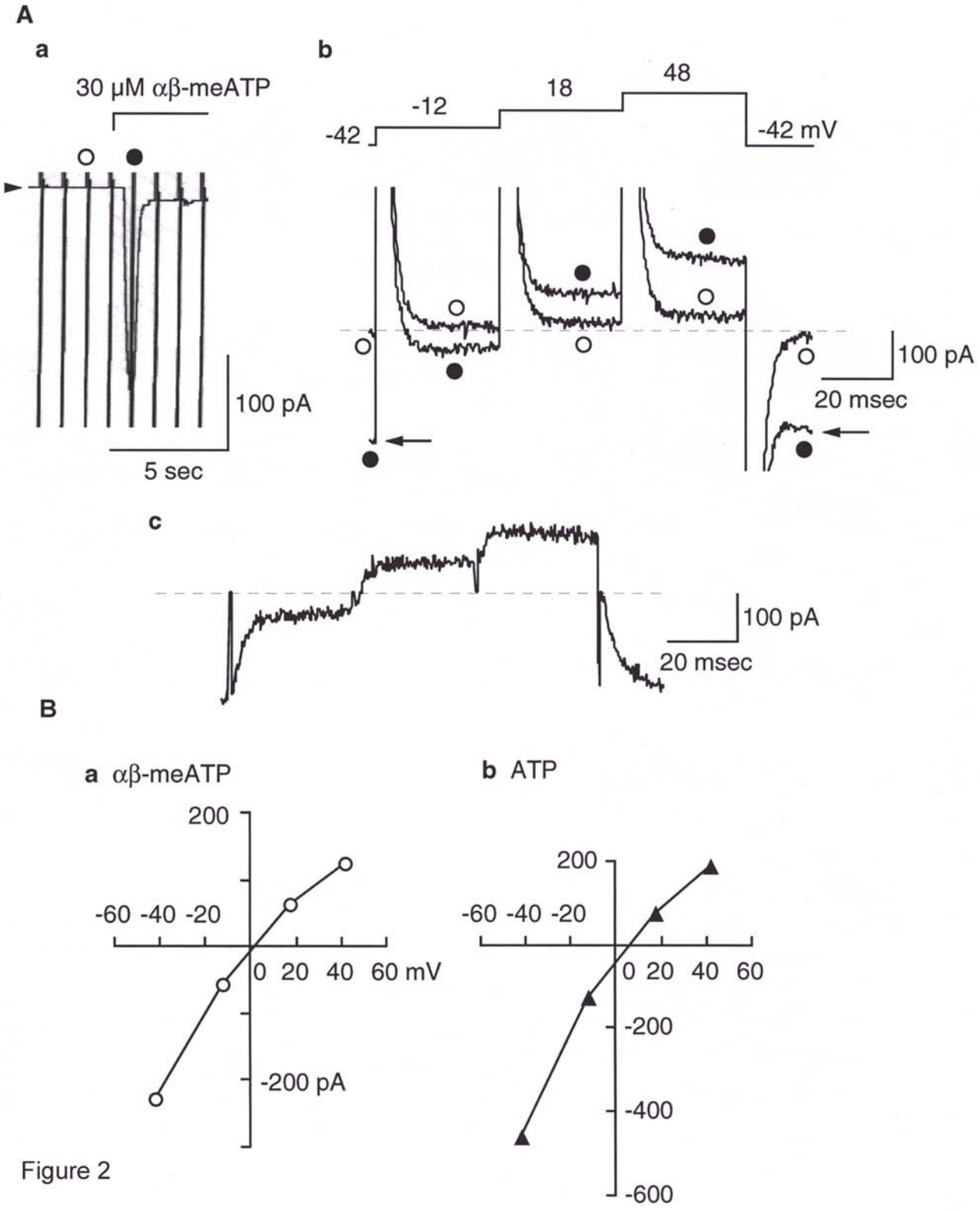
A
a
30 μM αβ-meATP
100 pA
5 sec
b
48
18
-12
-42
-42 mV
100 pA
20 msec
c
100 pA
20 msec
B
a αβ-meATP
200
-60 -40 -20
0 20 40 60 mV
-200 pA
b ATP
200
-60 -40 -20
0 20 40 60
-200
-400
-600

Figure 2

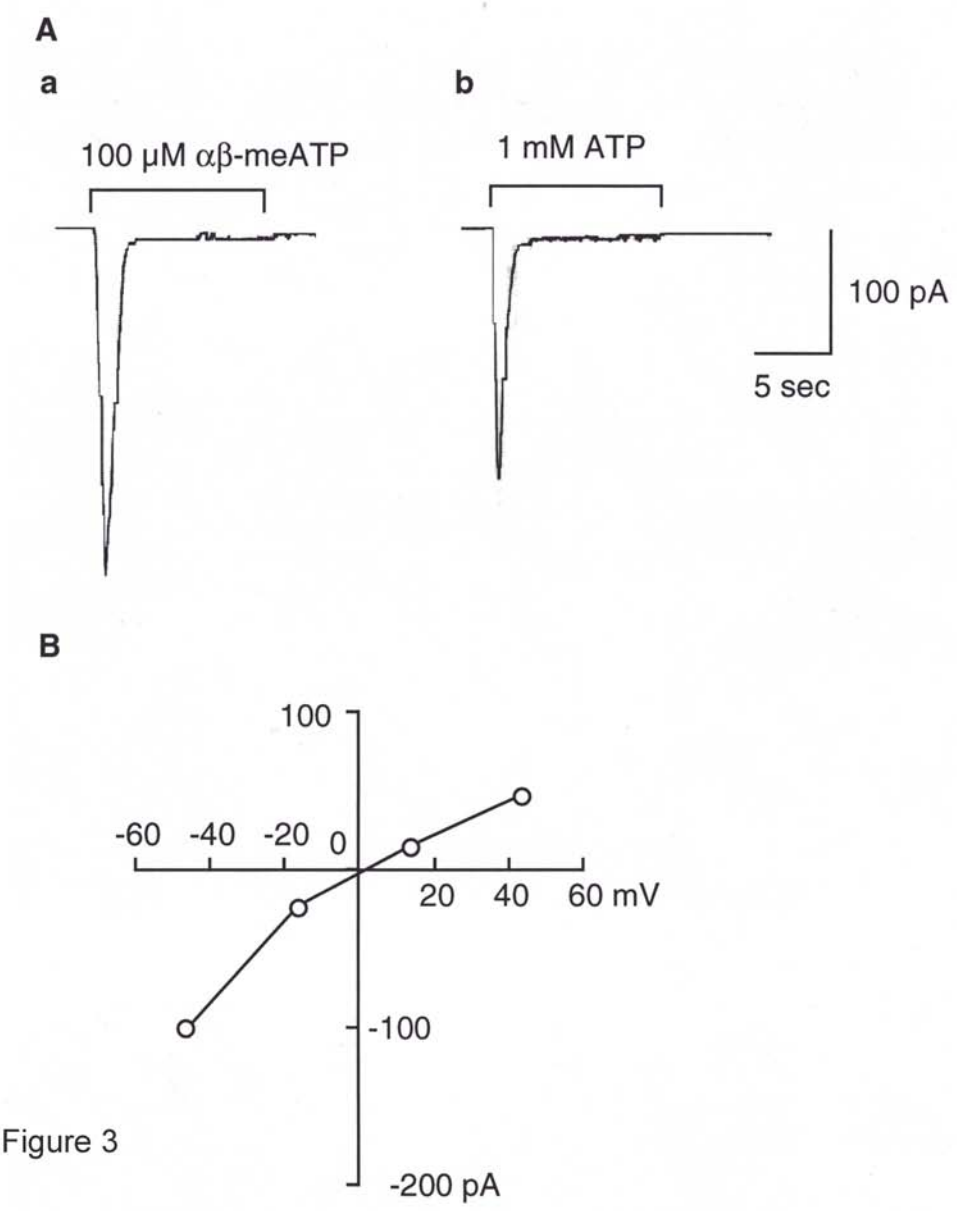
A
a
b
100 μM αβ-meATP
1 mM ATP
100 pA
5 sec
B
100
-60
-40
-20
0
20
40
60 mV
-100
-200 pA

Figure 3

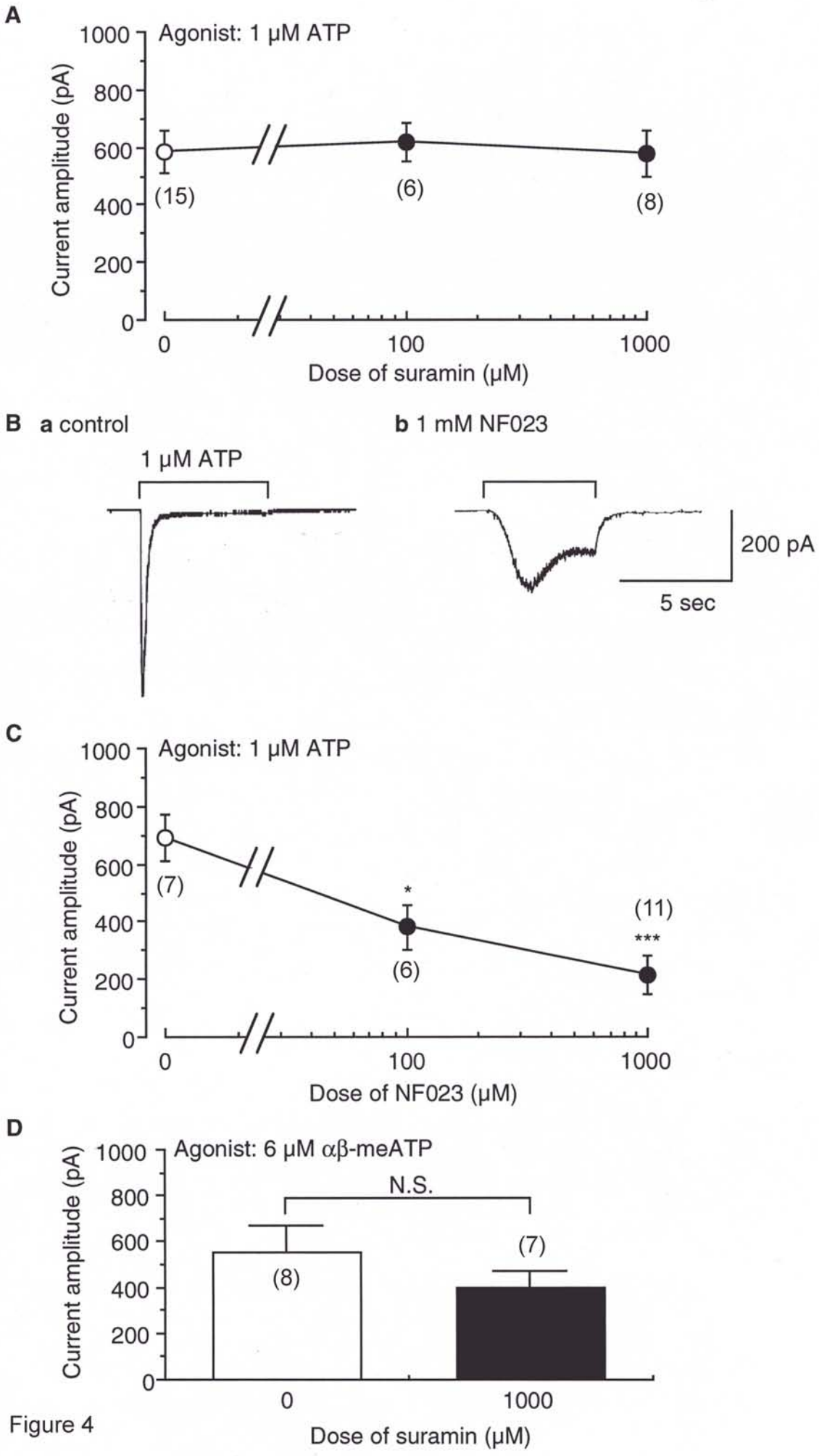
A
Agonist: 1 μM ATP
Current amplitude (pA)
1000
800
600
400
200
0
(15)
(6)
(8)
0
100
1000
Dose of suramin (μM)
B
a control
b 1 mM NF023
1 μM ATP
200 pA
5 sec
C
Agonist: 1 μM ATP
Current amplitude (pA)
1000
800
600
400
200
0
(7)
*
(6)
(11)
***
0
100
1000
Dose of NF023 (μM)
D
Agonist: 6 μM αβ-meATP
Current amplitude (pA)
1000
800
600
400
200
0
N.S.
(8)
(7)
0
1000
Dose of suramin (μM)

Figure 4

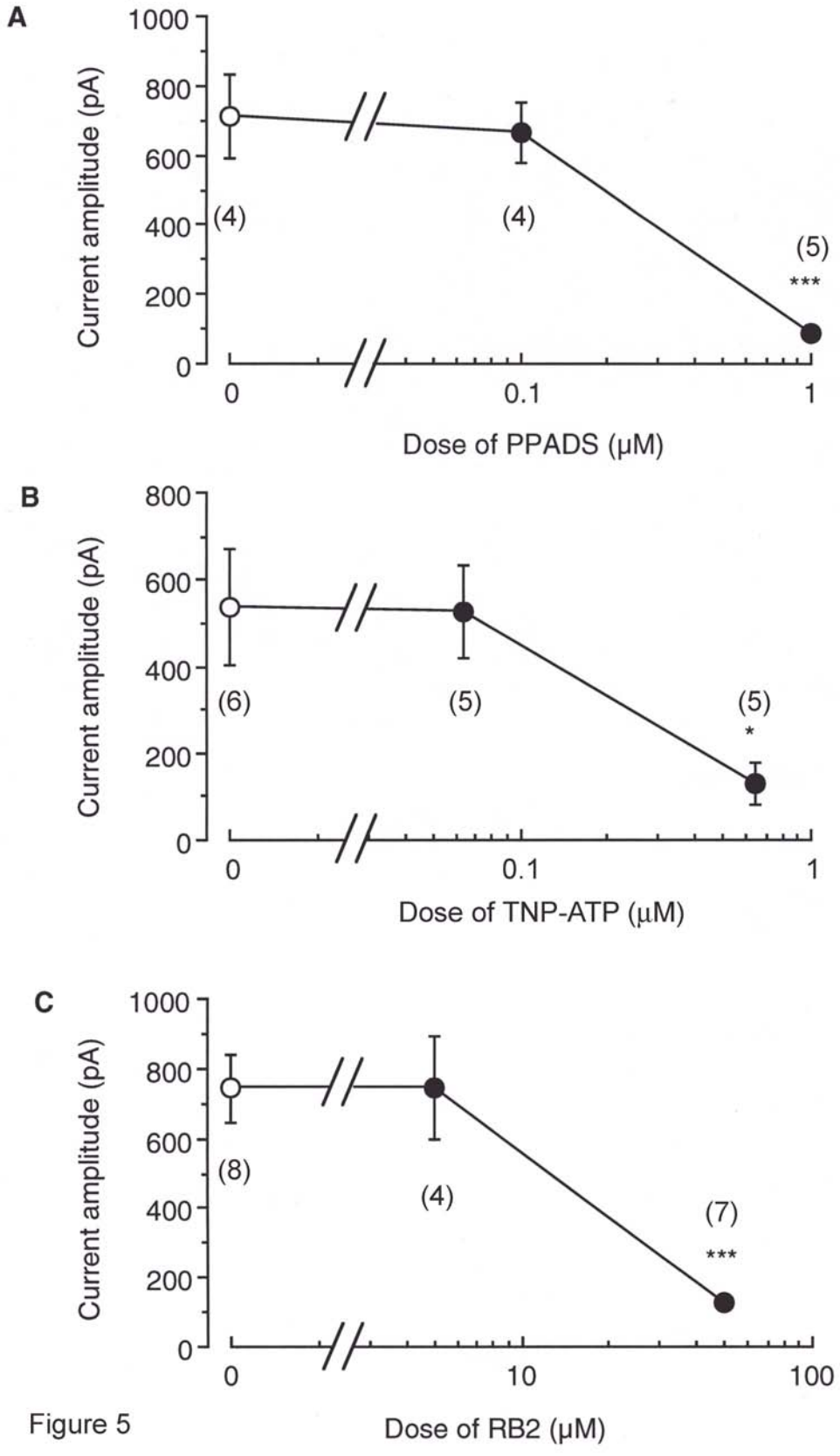
A
1000
800
600
400
200
0
Current amplitude (pA)
(4)
(4)
(5)
***
0
0.1
1
Dose of PPADS (μM)
B
800
600
400
200
0
Current amplitude (pA)
(6)
(5)
(5)
*
0
0.1
1
Dose of TNP-ATP (μM)
C
1000
800
600
400
200
0
Current amplitude (pA)
(8)
(4)
(7)
***
0
10
100
Dose of RB2 (μM)

Figure 5

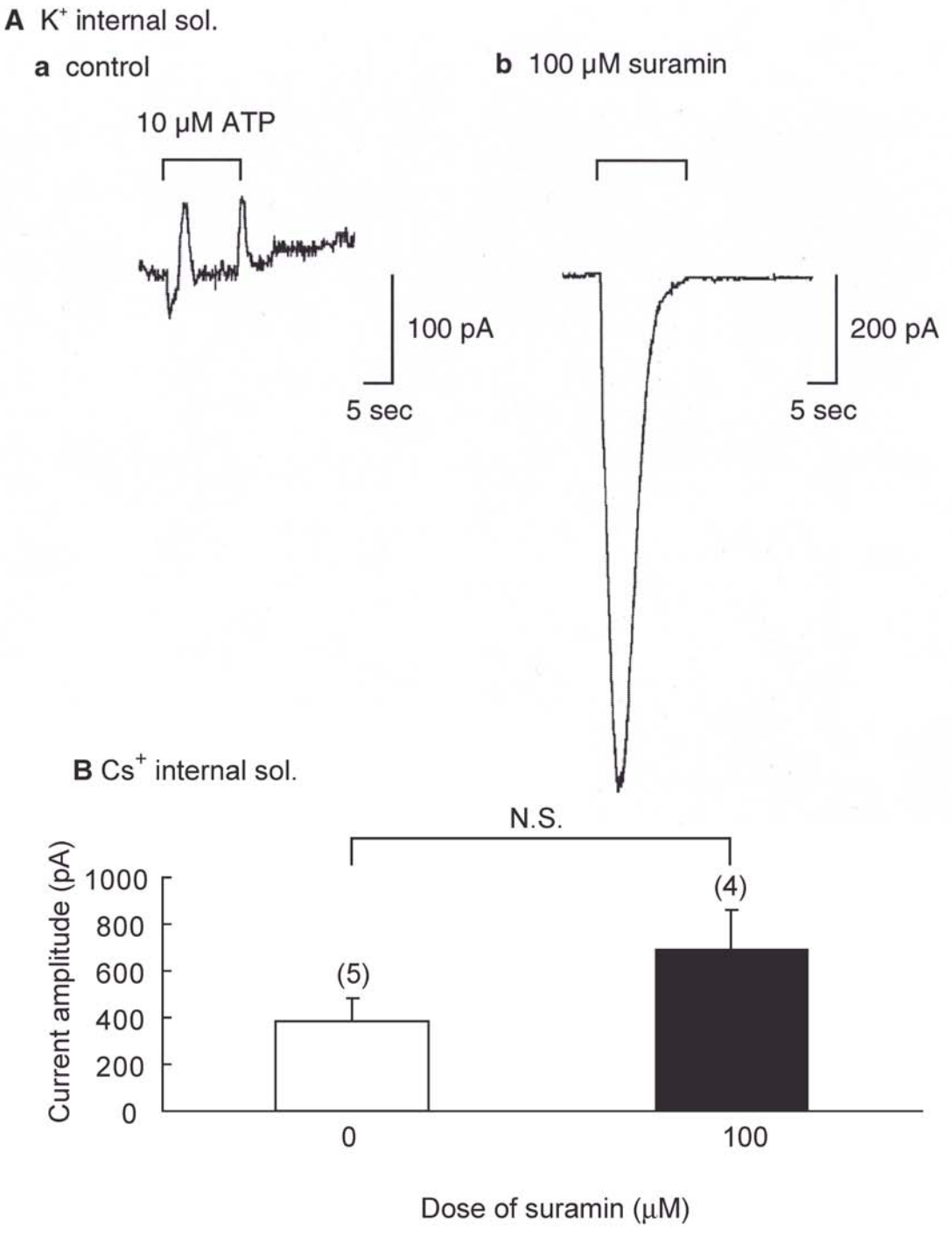
A K+ internal sol.
a control
b 100 μM suramin
10 μM ATP
100 pA
5 sec
200 pA
5 sec
B Cs+ internal sol.
N.S.
Current amplitude (pA)
1000
800
600
400
200
0
(5)
(4)
0
100
Dose of suramin (μM)

Figure 6